TURBULENT HEATING AND COMPRESSION EXPERIMENTS IN B.M.E. II (BERKELEY MIRROR EXPERIMENT II)

by

H. deKluiver

Memorandum No. ERL-M240

7 March 1968

ELECTRONICS RESEARCH LABORATORY

College of Engineering
University of California, Berkeley
94720

Research sponsored by the National Science Foundation under Grant GK-738 and the Electronic Technology Division, Air Force Avionics Laboratory, Wright-Patterson Air Force Base, Ohio under Contract AF33(615)-3524.

TABLE OF CONTENTS

ACKNOWLEDGEMENT

The author hopes to contribute with the experimental work described in this report to possibilities for a better continuation of the turbulent plasma heating and compression experiments in BME II. The author was on leave from September 1965 to March 1967 from the FOM-Institute for Plasma Physics, Rijnhuizen, Jutphaas, The Netherlands.

Special thanks are due to Professor Alvin W. Trivelpiece for the suggestions of this experiment. I could learn very much of his excellent experimental skill. His friendship has been appreciated.

Special thanks are also extended to Professor Allan J. Lichtenberg for the many suggestions for measurements and his critical comments during the diagnosis of the experimental phenomena.

I am grateful to my friend and colleague visitor Professor Tatsuo Kawamura from Japan for the pleasant cooperation during the first experiments.

The work could not have been carried out without the skill and enthusiastic help of Mr. George Conklin, Mr. John Benasso, Mr. Luigi Graziano and Mr. Orwin Westwick.

Finally, I am grateful for the pleasant contact with colleagues and students.

I would like to gratefully acknowledge the financial support for the travelling expenses by the Fulbright Organization.

Similarly, the support granted by the Electronics Research Laboratory is sincerely appreciated.

INTRODUCTION

In recent years considerable interest has been shown in turbulent plasma heating. Experimental work has been mainly performed in Russia.[1] The theoretical understanding of the phenomena associated with a turbulent state of a plasma is still far from complete. One way of approach is starting from the Vlasov equation with a nonlinear damping term.[2] The actual turbulent state is also considered by Kraichman's method which predicts a characteristic noise power spectrum similar to hydrodynamic turbulent spectra (Komolgoroff spectra).[3]

In actual experiments links between experimental results and theory are found by the scattering of unstable electron-ion two-stream instabilities in times of 20-100 x $(\omega_{pe})^{-1}$, resulting in a rapid quasi-thermalization as described by Buneman, Dawson and others.[4] Stated another way: when plasma is exposed to sudden increases in electric field strengths the plasma exhibits an anomalously high resistance. In very short times (10^{-7}-10^{-8}sec) considerable energy is taken out of the electric field and distributed among many degrees of freedom of electrons as well as ions.

The aim of the turbulent heating experiments in BME II is to increase electron energy and if possible, the initial ion energy, to obtain higher temperatures for both components after compression.

DISCUSSION OF THE INTENTION OF THE CAPACITOR HEATING EXPERIMENT IN BME II

As stated in the introduction one goal was to preheat the ions after injection of the plasmoid. Though the ion energy in BME I was never measured directly after compression, absence of neutrons indicated that energies of the ions remained below 1 keV. One possibility was that the initial ion energies were limited by the vessel radius ($R \approx 5$ cm) at the moment that the plasmoid occupied the available mirror field region. However, from end loss analysis (127^{o} analyzer) of the longitudinal ion energies it was inferred that ions of considerable energy (see Fig. 13) are present initially. Those ions are not effectively trapped by the rising field. Moreover, it was found later as will be shown in section 7 in more detail that due to the effects of cold gas from the walls and the source the more energetic ions are replaced by colder ones. From time of flight considerations it has been found that the bulk of the plasma fills the mirror region in approximately 10 μsec. Taking the mirror region length to be 10 cm, yields, for the average thermal speed of D^{+} ions, 10^{6} cm/sec, corresponding with ion energies of 1 eV. At this time, when almost all energetic (> 10 eV) ions have disappeared,the compression ratio lies in the range of 100 - 200. Final ion energies of some hundreds of eV could be explained in this way.

In the planning stage of the turbulent heating the line of thought

was as follows: Try to employ turbulent heating to increase the initial energy of the ions (1 eV) to such an extent that the maximal ion energy determined by the vessel radius could be obtained. Only a moderate effect was needed to achieve this. For B $\approx$ 250 Gauss, ions up to 30 eV could be contained; thus heating from 1 eV to 30 eV was needed which after compression by a factor of 200 would lead to final energies of a few keV's. Furthermore, if the moment of switching the capacitor voltage to the plasma is chosen such that the imposed frequency of the oscillating current would match the ion gyration frequency in the magnetic mirror region, at that time, it was hoped that ions could be heated by an induced ion-cyclotron instability. The naive picture was that a bunching streaming electron cloud in the vessel centre could give a large radial electric field seen by the ions at the ion cyclotron frequency - this giving rise to large $\frac{E}{B}$-drifts. Another possibility for heating, by means of a longitudinal oscillating discharge through the plasma, involves the mechanism of an electron-ion two stream instability.

The apparatus is shown schematically in Fig. 1. The oscillatory discharge is drawn between the two central electrodes situated slightly outside of the positions of maximum magnetic field. The pulsed plasma source is located in one electrode.

THE BME II MIRROR FIELD

For a better knowledge of the compression ratio of the trapped plasma, and to know the relation between the oscillator discharge frequency and the cyclotron frequency at the time of the onset of the induced instabilities, it was decided to determine the BME II mirror field, accurately, as a function of position and time. For this purpose a rod with a large number of coils ($n \times A = 50\ cm^2$; $RC = 10^{-2}$ seconds) was placed along the axis of BME II. The $\frac{d\varphi}{dt}$ signals have been integrated by a tetronix 0-unit. From the coil constants the magnetic field was calculated.[5]

The results are presented in the following figures: Fig. 2 gives the general shape of the magnetic field, as function of position with respect to upper and lower copper coils, taken at a time near the field maximum. The numbers indicate the position of the probe coils during the measurements and are spaced one inch apart. The two curves with numbers 294 H and 356 H correspond with two different bank settings. Fig. 3 shows the peak field in Gauss measured in the midplane as function of bank setting. Fig. 4a, b, c, d and e give the field as function of time. To obtain an indication of the non-adiabaticity of ions by the large rate of change of the magnetic field at early times from the data of Fig. 4 an appreciation number has been deduced. A parameter describing non-adiabaticity is: $\alpha = \frac{eB^2}{m} / \frac{\Delta B}{\Delta t}$. When $\alpha < 10$ the losses out through the mirror may be appreciable. In Fig. 5, α has been

given as function of magnetic field and the times corresponding to the field. It is clear that up to 10 μsec important losses due to non-adiabaticity may occur. The effects of non-adiabaticity are particularly important for those ions which have transit times $\frac{2\pi}{\omega}$ sec. Thus ions above some 20 eV longitudinal energy may be adiabaticly deflected into the loss cone.

TURBULENT HEATING OPERATION OF BME II

The experimental arrangement is shown schematically in Fig. 1. The plasma forms an impedance parallel to the external LC-circuit. This LC-circuit oscillates after a double spark-gap switch has been triggered. Via a transmission line (coaxial cable) voltage is brought between plasma source which serves as the upper electrode and an opposite electrode in contact with the vessel wall. The ground side of the coax cable has been connected to the vessel wall. The plasma source is insulated from the stainless steel chamber by an alumina cylinder. The position of the plasma source and the other electrode was chosen 1 inch outside the mirrors. The lower electrode cylinder has a hole on top so that escaping particles fluxes could be examined by different diagnostic tools.

The plasma source was operated usually at low voltages i.e. 3 kV on a trigger electrode and 2 kV on the main electrode of the source. At higher voltages the plasma flux becomes excessive, with a corresponding high neutral gas pressure (10^{-4}-10^{-3} Torr) resulting from plasma hitting the vessel wall. With a 2 μF, 40 kV capacitor oscillations at 240 kc/sec and 340 kc/sec have been obtained depending on the inductance of the shorting circuit used. Other capacitors used were 1 μF, 10 kV at 390 kc/sec and a fast capacitor 0.1 μF, 20 kV at 1 and 2 Mc/sec. (In the case of the fast capacitor a tunable low inductance cicuit was used by varying the lengths of the shorting circuit strips.)

The voltage between plasma source and opposite electrode was measured by a 1/200 voltage devider. Currents through the plasma were measured by a Rogowsky-type flux loop in the "hot" side of the transmission line followed by 0-unit integration. The Rogowsky-loop was calibrated, for the frequency ranges used, by an external current source. The calibration figure was 0.4 mV/Ampere for the setting Z_i = 0, 1 MΩ Z_f = 0.001 μF of the Tektronix 0-unit. The current measurements do not give the partition of currents flowing from plasma source to lower electrode and wall respectively. The time of initiating the plasma source, magnetic field, and the heating capacitor discharge could be chosen at will by the setting of time delay circuits.

The choice of the plasma as an impedance parallel to the external circuit rather than as part of the circuit stems from the philosophy to have an oscillatory voltage of prefixed frequency impressed on the plasma - thus the circuit frequency determined by the external self-inductance and not by the variable properties of the plasma itself. In this respect the arrangement differs somewhat from the linear Russian experiments where the plasma is directly part of the circuit.

One good timing sequence for plasma trapping was found to be that in which the plasma source was switched 2 - 5 μsec before the magnetic field started to rise. The heating capacitor was switched from 1 to 30 μsec after the field depending on the type of experiment.

A SHORT DESCRIPTION OF THE DIAGNOSTIC TOOLS USED

The different diagnostic instruments will be briefly discussed. Results are given in later sections when the experimental findings are described.

A. Vacuum UV and UV Light Emission of the Plasma

The light emission of the hydrogen plasma as a function of time gives information about the presence of neutrals during compression. To investigate the light emission a McPherson vacuum monochromator (0.5 meter) could be connected via a flexible pipe connection to one of the 1 cm central diagnostic ports. Behind the exit slit a sodium salicylate covered PM tube converted the UV into visible light. Data were taken in the spectral range between 400 Å and 6500 Å.

B. Measurement of Radially Escaping Neutrals

Two diagnostic techniques have been used

1) a 90^{o} Be-Cu secondary emission detector;

2) a Bendix open particle multiplier.

1) The 90^{o} Be-Cu detector.

At the end of a radial port a Be-Cu detector was mounted with its axis along that of the port. The cone shaped top of 90^{o} was facing the plasma. Secondary emission coefficients between 1 - 2 can occur

for neutrals of a few hundred eV. The secondary electrons would be collected on a cylinder surrounding the Be-Cu cone. Usually the Be-Cu cone was biased at - 50 volts. Sacrifying speed of detection, using 1 MΩ at the scope a signal of approximately 5.10^{-10} A could be measured. A plasma volume of 0.1 cc. could be seen with a solid angle of approximately 10^{-5} sterradians. For this geometry, taking a value of $\langle \sigma v \rangle$ of 10^{-10} cm^3/sec; for ions of 100 eV, for charge exchange, the product $n_o n_+ = 10^{26}/cm^6$ could be measured. n_o is the neutral particle density per cm^3, n_+ the ion density. Under somewhat more favorable conditions for the plasma volume and a $\langle \sigma v \rangle$ value for ions near 1 keV the limit of the detection could be $10^{24} - 10^{25}/cm^6$. The use of this detector was thought to be marginal for the estimated figures of $10^{12} < n_+ < 10^{13}$ and $n_o \approx 10^{12} cm^{-3}$. But the simplicity of the detector construction made the attempt worthwhile. A disadvantage of this collector is its sensitivity ot vacuum UV light. Apart from the strong light emission during the first 20 μsec, giving photoelectrons, no signal could be observed.

2) A Bendix open electron multiplier, having a gain between 10^7 and 10^8, was used, after the Cu-Be detector was found to be too unsensitive. A description of this pultiplier can be found in the literature[6]. The multiplier is sensitive to neutrals as well as to vacuum UV radiation. The sensitivity to neutral-charge exchanged particles depends strongly on the energy of the particles.[7] For

deuterium atoms the secondary emission coefficient on the tungsten surface is not known exactly, but very probably increases rapidly from roughly 0.1 near 100 eV to a value larger than 1 near 3 keV. The multiplier is sensitive to radiation between 2 Å (6 keV photons) and 1500 Å. Peak quantum efficiency is 10 percent. To distinguish between particle and photon signals a turnable wheel with 1 cm holes was put in fromt of the multiplier. The holes were used open, with small pinholes and with a quartz window and a LiF window. Aluminum foils of 17 μ and 1 μ have been used; gold foils of < 0.5 μ were used. It was found possible to discriminate against radiation with these windows.

The Bendix was placed in front of a radial port. The Bendix housing was evacuated by an ion-sputter pump to 2×10^{-7} Torr. Dark current pulses at 2100 Volts were found at a rate of one per ten seconds. The pulses were broadened to 2 μsec halfwidth. Pulse heights amounted to ~50-100 mV. The voltages were adjusted following the data scheme belonging to the multiplier. Here again an estimated plasma volume of 0.1 cm^3 could be viewed by the multiplier at a solid angle of maximally 10^{-5}. To avoid saturation and "pile up" very small pinholes had to be used.

C. End Loss Detection of Ions

An Eubank-Wilkerson 127° electrostatic energy analyzer was used axially. The apparatus as used in the experiments is described

in the thesis of Zaviantseff.[8] The detection was of the Daly type. The secondary electrons from the aluminum disc (usually at -10 to -12 kV) behind the exit slit of the analyzer were collected on a plastic disc covered with a thin aluminum layer at ground potential. The plastic disc had optical contact with a RCA PM-tube. This small PM-tube had to be used at 1200 Volts for proper operation. Under these conditions single-ion pulses heights are between 50 and 100 mV.

The analyzer was used end-on to monitor ion end losses. To investigate possible influence of strong magnetic field on the operation it has been used at approximately 0.5 and 2 meters distance from the lower mirror. The relative intensities as function of time were essentially the same at different distances. A disadvantage of the analyzer is its insensitivity for ions below 100 eV. To enable ions of small energy to escape longitudinally by increasing the nonadiabaticity a shorted loop with an extremely long L/R was installed downstream (Forsen's thesis).[9] As Forsen remarked, the effect of nonadiabaticity is probably not yet sufficient; i.e. it may be that most of the escaping ions still follow the field lines not entering the entrance slit of the energy analyzer. This may be an explanation for the absence of ion signals in the appropriate energy range when the magnetic field had values of some kilogauss.

A less sophisticated, but more successful detection method for both ions and electrons, in the low energy range (a few eV to 200 eV),

was a simple biased collector disc. The disc was placed one centimeter below the hole in the lower electrode. The bias potential on the collector was varied from - 200 to + 200 Volts, to obtain either ion or electron saturation. The net current was measured as a voltage across several resistance values, the resistance being chosen to give a suitable voltage drop at a given current.

D. Synchotron Radiation Measurements

With the synchotron radiation detector,[10] time resolved, but spectrally unresolved, radiation was examined through one of the radial ports. Measurements were taken with and without the heating capacitor. The intensities, averaged over many shots were compared in the two circumstances to obtain a rough measure of electron heating and changes in electron density.

E. X-ray Emission of the Plasma

As a measure of the electron temperature the X-ray Brehmstrahlung spectrum at energies above kTe was investigated. The X-ray detector consisted of a PM tube, in front of which a CsI commercial type scintillator was placed in optical contact. The PM tube scintillator-collimator was placed, in most of the experiments, facing a transverse diagnostic port. This port was closed by a 3 mm quartz window. The PM tube output pulses after some integration to a 2 a 3 μsec halfwidth were either read directly from photographs or connected to

a pulse height analyzer of Nuclear Data Instruments. The pulse heights were calibrated with the 30 and 660 keV peaks of a Ce^{137} sample.

Temperatures could be derived from the pulse height data comparing the slope of integrated pulse count plots vs energy with computed curves.[11] In general, 50 shots of 1 millisec counting time were sufficient to obtain a reasonable temperature determination.

F. Neutron Counters

The presence of any flux of neutrons for the peak densities of 10^{12} - 10^{13} part/cm^3 in the experiment would give a lower bound on the ion temperatures reached. For this reason measurements have been taken with a PM tube LiI crystal and polyethelene moderator combination. Pulse heights of this combination were tested in Nuclear Engineering with a plutonium 238 berylium stable isotope source, giving neutrons between 3 and 5 MeV at a rate of 10^7/sec. Measurements of the pulses taken with this combination - PM tube at 2100 volts in 1000 ohm load are shown in Fig. 6. Also observations with a 1 liter plastic scintillator, PM tube, combination were carried out. No neutrons have been found during the BME II experiments.

ELECTRON CURRENTS AND ELECTRON HEATING WITH THE CAPACITOR DISCHARGE

This section is devoted to the description of the major results of the experiments. In the next section results of measurements will be presented which extend the picture obtained here. Results with the 2/μf capacitor at 240 and 340 kc/sec and 1/μf capacitor at 390 kc/sec are described in this section.

When a damped oscillating current is applied to the plasma at the frequencies given above, and at appropriate times with respect to the rise of the magnetic field, a considerable increase in X-ray density as well as the pulse heights has been found, as will be shown later in this section. The effects were marked when the following timing sequence is followed. Plasma injection starts 1 to 5 μsec before the magnetic field begins to rise. For 240 kc/sec a switching of the capacitor between 2 and 4 μsec after the magnetic field gave the strongest heating effects. For 340 and 390 kc/sec a maximum effect is found between 5 and 7 μsec after the field. A variation of the rise time of the magnetic field required a shift of the capacitor delay to such a value that the same magnetic field was found at the time of application of the capacitor. At first it was thought a relation existed between the value of the magnetic field at the time when the heating capacitor started to oscillate and the oscillator frequency. The idea was that a close correspondence might exist between the applied frequency and

the ion cyclotron frequency at the moment of switching, the frequencies being nearly the same. By a better measurement of the magnetic field with emphasis on the accuracy at early times (see Fig. 2 to 5) this assumption was found to be invalid. Moreover, for other reasons it was found that this idea is wrong. At the moment of triggering the heating capacitor the plasmoid does not connect the source and the opposite electrode. This is found from signals on the end loss detector as is shown in Fig. 7 where it can be seen that plasma contact starts to be appreciable after approximately 7 μsec, being optimal near 13 μsec and degrading in roughly 20 μsec due to the compression. The effects of the capacitor on the plasma is best illustrated by current and voltage photos as function of time. For the 240 kc/sec and 340 kc/sec cases examples are given in Fig. 8 and 9.

It has been found for both frequencies that a first current peak occurs between 10-13 μsec, i.e. when B ≈400 Gauss for both 240 kc/sec and 340 kc/sec. Certainly the minimum times for the first current peak must be related with the time that plasma contact is established between the electrodes, but an indirect effect of the magnetic field is shown by the experiment previously mentioned where the rise time of the magnetic field was varied a considerable amount. Shifts of up to 7 μsec to later times in the moment of switching the heating capacitor, had to be used to obtain identical heating effects at the lowest fields. It is suggested that the influence of the occurrence of the magnetic field

may be that its value regulates the density of the plasma at which the heating currents can develop. In Fig. 8 a voltage-current example is given for 240 kc/sec. The bottom trace of Fig. 8 shows the voltage between plasma source and opposite electrode damping out in the absence of plasma. Middle and upper traces have been taken in the presence of plasma, showing respectively current through and voltage across the plasma. At 13 μsec (B = 400 G) a fast rising current peak appears in phase with the voltage (middle and upper traces); resistances are in the order of 1 ohm. It can be seen that the voltage is decreased considerably due to the charge consumption in the first spike. After that, voltage and current are almost 90^{o} out of phase, damping out with the unperturbed time constant.

At 340 kc/sec current and voltages traces are given in Fig. 9. Between 10 and 13 μsec the ohmic type current spikes occur, as can be seen from the collapse of capacitor voltage maxima following. The whole picture is certainly more wild than in the 240 kc/sec case. Apart from the "regular" small current phenomena (currents roughtly 100 A or so) asymmetric current spikes of 10-30 kA occur at distances decreasing with increasing time, indicating some dependence of the oscillations within the plasma on the magnetic field. The oscillations are not always present. When present, they are accompanied by stronger X-ray emission. No explanation has been found for these oscillations.

Neither currents nor heating was found when the fast (1 to 2 Mc/sec) capacitor was used. A wide range of timing sequences between discharging the plasma source, discharging of the capacitor and the start of the rise of the magnetic field were used in those experiments. If a relation between ion cyclotron frequency and the applied frequency must exist for the heating effects, then the absence of any heating could be explained by the effect that at times corresponding to those frequencies the adiabatic compression had already broken the contact between the plasma and the electrodes. For 1 Mc/sec the corresponding magnetic field is 1200 Gauss; the time is 21 μsec. At that time plasma contact is marginal. Moreover the plasma density might be unfavorably high for collisionless heating, any instability being quenched by collisions.

Pulse height analysis of the X-rays observed transversly indicated strong heating of a part of the electrons of the plasma, for the lower ringing frequencies. In calculating the temperature it is assumed that the bremsstrahlung arises from electrons hitting a thick target (the vessel wall) but the temperature would not differ significantly from plasma bremsstrahlung.

Without additional heating, electron temperatures of 50 keV are found from X-ray scintillation measurements. Also electron synchotron radiation has been measured transversly, spectrally unresolved, to obtain a measure of nxT.

The deductions from the slope of the increase in the synchrotron radiation with time were inconclusive in determining the plasma

temperature. (However, at the moment of these measurements the magnetic field as function of time was not available with precision. Also the response of the Putley detector as function of frequency for the higher harmonics of the synchrotron radiation is not known too well).

An example of X-ray and synchrotron signals and the large influence of the heating capacitor is given in Fig. 10 a) and b). Notice that the plasma is stable, as it nearly always is, with X-rays persistent longer than 10 msec. Stable is defined here by the absence of singular X-ray bursts, occurring when plasma hits the wall.

Integral pulse counts from 50 runs compiling X-ray scintillations during 2 msec after peak compression are shown in Fig. 11 a without external excitation and in Fig. 11 b and 11 c for respectively 240 and 340 kc/sec oscillations. The slopes are almost proportional to 1/kT, where T is the electron temperature. In Fig. 11 b and 11 c the curves no longer represent a single Maxwellian distribution. If an approximation into two straight line parts, representing nearly Maxwellian distributions, is made, the following results may be derived. For 240 kc/sec oscillations 57 percent of the electrons have an equivalent temperature of 140 keV with 43 percent at 60 keV. The effect is stronger for 340 kc/sec where 37 percent reach 240 keV and 63 percent of the electrons correspond to 60 keV. (Integral pulse counts extrapolated to zero energy are taken proportional to $N/(kT)^{1/2}$; thus it has been assumed that the X-ray production is from electrons hitting the "thick target" wall). Notice

that, although the fraction of heated electrons is somewhat smaller, more intense heating occurs with the 340 kc/sec capacitor than with the 240 kc/sec capacitor.

Synchotron radiation is considerably enhanced with heating. An average over 20 shots yields an increase of a factor of 4 for 240 kc/sec and a factor of 9 for 340 kc/sec oscillation. These results are not inconsistent with the X-ray data. If one forms the n × kT product for the fraction of heated electrons, one finds an increase of 2.2. Also the integral pulse count is a factor of 3.5 larger for the unheated electrons with the capacitor. If one takes this number proportional to N the total heating effect should have been a factor of 7.7. A better correspondence could hardly be expected.

In conclusion it can be remarked that a faster rise time of the electric field seems to increase the temperature of part of the electrons. Its dependence on the E-field has to be investigated over a wider frequency range.

To explain the anomalous - large - resistance during the first current peak of approximately 1 Ω the idea of an electron-ion two-stream instability in a non-linear regime might be used. If one uses the proposed mechanism of Babikin et al[1] for a similar situation, an expression for the "resistance" is formally found: $R = L\,(\epsilon_o \omega_p S)^{-1} (M/m)^{-1/3}$, with L the electrode separation (0.15 m), S the plasma cross section (roughly the electrode surface 0.05 m^2) and a plasma

density of 4×10^{16} el/m^3, a value of 2 Ohm is calculated, in reasonable agreement with the experimental data. See also the paper of Buneman.[4]

From the compression ratio 100 at the first breakdown peak, an energy gain per particle between 1 and 2 keV is found consistent with the voltage across the electrodes.

The values taken above are, however, a factor of 5 too low to explain the currents of 500 A. However, part of the current from the plasma gun electrode might also have hit the wall so that in fact the plasma area could have been somewhat larger.

OTHER OBSERVATIONS ON PLASMA DENSITY AND TEMPERATURE

An important part of the investigations was to determine whether ion heating occurred due to the oscillating current. We first present the results, followed later by typical measurements supporting the ideas presented.

It has been found that the bulk of the plasma ions at peak compression have energies of a few eV's to approximately 100 eV. The number density is approximately 10^{12} ion/cm^3 in a volume less than one cm^3. No effect of the capacitor discharge on this energy distribution has been measured near peak compression. To explain this, the initial trapping processes were investigated in greater detail. From our preliminary measurements there is an indication that the capacitor discharge produces some initial ion heating at times earlier than 60 microseconds. However, more detailed measurements are necessary in the difficult energy range up to 100 eV. An ExB-ion analyzer seems to be the best method for making such measurements. The absence of appreciable (keV) ion energies near peak compression time ($\approx$ 500 μsec) can be explained as due to several effects: ionization of cold gas, charge exchange losses, and non-adiabaticity of the hotter component in the early period of the compression (the first 60 μsec).

To test whether any substantial number of ions attained temperatures above 3 keV (as seemed possible from vessel dimensions, properties of the plasma source, magnetic compression rates, etc.), neutron detectors

have been used. The results were negative. From the absence of neutrons one can conclude that, for a density of 10^{12} ions/cm^3, the ion energies are below 3 keV.

With the 127° ion energy analyzer used end on, measurements have been carried out between energies of 100 eV and 30 keV. An example is given in Fig. 12. Except during the first 60-80 μsec, no longitudinal ion losses have been found usually. Several maxima can be found during the first 80 μsec. Later smaller peaks near 100-120 μsec may be due to an instability during compression. Those peaks are not always present and may be correlated with similar maxima in synchotron radiation. Low energies might not be detected, however, due to the adiabatic expansion of the end loss ion flux and relative insensitivity of the ion analyzer below 100 eV. This may explain the absence of signals at later times. An energy analysis pertaining to escaping ions of the plasmoid at about 15 μsec is given in Fig. 13.

For discrimination against soft X-rays and vacuum UV light, when a Bendix multiplier is used, the spectrum has been investigated in steps of 50 Å from 400 to 1200 Å with the McPherson monochromator. Apart from a weak continuous background, strong lines, some from impurities, have been found near 1215, 1032 and probably 765 Å. The lines are identified as Lyman α and tentatively as O_{VI} and N_{IV}, respectively. The most important conclusion, however, is that after 60 microseconds negligible radiation is emitted in a large portion of the spectral

region where the Bendix multiplier has a high sensitivity for photons. A numerical estimate of the intensity of Bremmstrahlung of a plasma of density $10^{12}/cm^3$ and an electron temperature of 60 keV shows that the emission is not measurable in this spectral region. The intensity profile shows (at least) two peaks near 20 and 60 microseconds. This is illustrated in Fig. 14 for the Lyman α line.

From the absence of monochrometer signals after 60 microseconds, we infer that the signals from the Bendix multiplier at later times are due to charge exchange neutrals escaping transversally. (See also Appendices I and II). Studies of transmission through aluminum foils of different thickness (1, 2 and 17 microns) and through a Li fluoride window confirm that only during the first 60 microseconds appreciable light emission exists in the spectral region of the Bendix. Transmission through 1 micron Al foil of 10 keV deuterons would be approximately 30 percent. The signal through a diaphram of 1 mm at 50 cm distance from the center was initially intense enough to saturate the Bendix, when trapping was good, and degraded into single spikes after several miliseconds. Instabilities often show upon the Bendix signal at the same time as an X-ray burst, but are not always correlated. On the average there appeared to be no change in the Bendix signal with and without the capacitor. Fig. 15 gives a typical Bendix signal through a small hole. Saturation of the Bendix can indeed be expected for apertures used, assuming charge exchange between neutral gas of pressure of 10^{-5} Torr and

3.10^{12} ions/cm^3 of 50 eV energy. Further energy discrimination with the Bendix is not possible without additional energy analysis. (See also Appendix I).

Additional energy analysis has been obtained with a simple Faraday-type collector used end-on. For ions of low energies, small variations in retarding voltage should result in large differences in collected current. Several maxima in the collected current can be found as a function of time. The sign of the current in the various maxima depends on the bias voltage applied to the collector. Currents up to 1 A have been measured. Application of small negative voltages stop the colder electrons at later times so that the ion current of the plasma source appears in the traces from 15 to 20 microseconds (see Fig. 16a). No influence of capacitor discharge on the magnitude of the first peak is found. After a period of no end losses there is a second burst of current at approximately 60 microseconds, the magnitude of which is a function of the applied bias voltage (see Fig. 16b). The current is negative for positive bias, (suppression of low energy ions) gradually reaching a saturation value near 100 volts. With the capacitor the end loss current is generally more strongly peaked at higher energies than without capacitor, so that some heating of the ions may be present at this early time. Currents up to 500 mA have been found. A plot of these observations for the peak near 15 microseconds together with the one near 60 microseconds is given in Fig. 17. More maxima in the loss current are found. A third and fourth maximum of progressively

smaller amplitude are found at 90 and 180 microseconds (see Fig. 16c).

The most important part of the collector current is that which gives the actual loss current of the trapped and compressed plasma. In Fig. 16d a specimen trace is shown at positive collector bias voltage. Peak values of the current are much smaller, approximately 0.5-2 mA. It can be seen that the current reaches its peak when the magnetic field has its maximum value. The decay time for the current is approximately 1.5 milliseconds (time for current to e-fold). At increasingly positive bias voltages the ions become more and more repelled and an electron saturation current is reached. For the negative biases the current reverses sign and has a smaller saturation value probably due to the hot electrons still present. Values of the negative current at peak compression versus positive bias voltage are given in Fig. 18. From the curve one deduces ion energies around 50 eV. No influence of the capacitor discharge has been found. Tentative explanation for the various early peaks in the electron current may be given as follows. The first maximum is explained as electron and ion currents arriving directly from the plasma source. The second peak may be explained as follows: at 60 microseconds the end loss detector sees the effect of ionization of neutral deuterium coming from the walls. Trapped electrons already heated somewhat by the compressing field strengths of several kG (electron temperatures of a few keV) ionize the gas front. Time of arrival checks with a distance of a few cm which the room temperature

deuterium must travel. The newly formed colder ions with recoil energies between 0.1 and a few eV's are better trapped by ambipolar fields than the original partially heated ions. Loss mechanisms due to charge exchange and non-adiabaticity are also more effective, the higher the ion energy. Consequently the colder ions with smaller energies are compressed. Their compression rate is only 20 to 40 times, so that the final energy of the largest part of the plasma remains low (tens of eV's). No correlation with the capacitor discharge can be expected under these conditions. However, the electrons are relatively little influenced during their heating by the ionization processes, so that, for the electron component, greater heating could be observed when using the extra capacitor discharge.

APPENDIX I

Charge Exchange Losses of 50 eV Ions as Measured by the Bendix

Although several factors are not known accurately we will attempt to find whether the saturation of the Bendix, up to several milliseconds after initiation of the magnetic field, may be caused by charge exchange of ions of 50 eV. The latter energy value is taken to be an average measure of the ion energies at peak compression as found from the end loss collector.

Suppose $n_o \approx 10^{-5}$ Torr $\equiv 4.10^{11}$ part/cc. From the end loss current and loss rate after peak compression, consistent with an ion energy of some 50 eV:

$$n_+ = 3 \times 10^{12} \text{ ions/cm}^3$$

$$\sigma_{cx} \approx 10^{-17} \text{ cm}^2$$

$$v_{ion} = 7 \times 10^6 \text{ cm/sec.}$$

The aperature of the Bendix is a 1 mm opening at 50 cm distance from the plasma. For the plasma volume contributing to the neutral stream we have typically V = 0.1 cc as seen by the Bendix. This leads us to a solid angle of $\Omega = \frac{10^{-2}}{4\pi . 2500} \approx \frac{10^{-2}}{31400} \approx 3.10^{-7}$ sterrad. The rate at which particles arrive at the Bendix is then: $\frac{dN}{dt} = V\Omega n_o n_+ \sigma_{cx} v_{ion}$. Substituting the above numbers yields:

$$\frac{dN}{dt} = (10^{-1}) \times (3 \times 10^{-7}) \times (4 \times 10^{11}) \times (3 \times 10^{12}) \times (10^{-17}) \times (7 \times 10^{6}) =$$

$$2.5 \times 10^{6} \text{ part/sec.}$$

The uncertainty in this number can easily be at least a factor of ten. If we accept a secondary emission coefficient below one for the neutrals - say 0.1 - (ref.) then the number of spikes per second could easily be larger than 2.5×10^{5} spikes/sec). With a half width for the separate spikes of 3 μsec this should lead to an integrated signal. This is what we also observe up to a few milliseconds after peak compression. With an amplification of 10^{7} for the Bendix setting used this yields a continuous current of at least

$$2.5 \times 10^{5} \times 1.6 \times 10^{-19} \cdot 10^{7} = 4 \times 10^{-7} \text{ Amp.}$$

This current over 1000 Ω would give signals in the order of 0.4 mV. With the above uncertainties, mainly in the residual gas pressure and plasma volume, this is not in contradiction with signals of 20 mV found in the experiment.

From the absence of Bendix signals through LiF we conclude no contributions of Lyman α light. When using the Al foils, apart from the first 60 microseconds, no signals appear. Using gold foils of approximately 0.2 micron also suppressed all Bendix signals. We are therefore led to the conclusion that the Bendix signal after 60 μsec is caused by a flux of neutral (or ionized) deuterium atoms of low energies. The absence of vacuum UV light on the Bendix as well as on the McPherson monochromator will be dealt with in Appendix II.

APPENDIX II

Bremstrahlung Radiation from the Plasma of the Cold Electron Component

Based upon the number for the cold plasma component found in the former appendix the contribution to continuous radiation (Bremstrahlung) in the sensitive region of the Bendix will be evaluated.

It has been generally found (see figure 14) that only, roughly speaking, during the first 100 μsec light emission can be measured by the McPherson monochromator.

Using 1 μ Al foil in front of the Bendix only shows some radiation during the first 60 μsec and absolutely no signal at later times. The radiation during the early tine has been scanned with the Mac Pherson monochromator. A few discrete lines have been found near 1215, 1032, and probably 765 Å. The lines are identified as Lyman α, O_{VI}, and N_{IV}. A weak continuous background is also present from 400 to 1200 Å. The Balmer lines are also present.

An estimation of the photon flux which could be seen by the Bendix will be made based on the earlier derived temperature of 50 eV and density of 3×10^{12} el/cm^3 for the colder electrons present.

The expression for the number of photons emitted in 4π sterradians, 1 cm^3, and per second is:[12]

$$\frac{dN_f}{d\nu} = cN_e^2 \left(\frac{\lambda_H}{kT_e}\right)^{1/2} g_f \frac{\exp\left(\frac{-h\nu}{kT_e}\right)}{h\nu} \qquad (1)$$

g_f is the Gaunt factor, taken equal to one here

λ_H is the ionization potential for hydrogen

N_e is the electron number density

T_e is the electron temperature

c is a constant, $c = 1.7 \times 10^{-40}$ erg cm^3.

Now we integrate (1) over the sensitive region of the Bendix, i.e. from 2 Å to 1500 Å. This gives

$$N_f = cN_e^2 \left(\frac{\lambda_H}{kT_e}\right)^{1/2} g_f \frac{1}{h} \left\{ -E_i\left(\frac{-h\nu_{min}}{kT_e}\right) + E_i\left(\frac{-h\nu_{max}}{kT_e}\right)\right\} , \qquad (2)$$

where $E_i(x)$ is the error function with complex argument.

Now we take $T_e \approx 50$ eV and $N_e = 3 \times 10^{12}$ el/cm^3. This gives a photon flux of $N_f = 1.7 \times 10^{11}$ photons/cm^3/sec in 4π sterradians. Taking for the Bendix aperture 1 cm^2 at 50 cm, a plasma volume of 0.1 cm^3 and an average quantum efficiency of 0.05 percent we find 7000 spikes/sec at the Bendix. Thus from the cold plasma electrons we could expect some 7 spikes/millisecond. This is a marginal number to be observed. Our experimental conclusions that the Bendix signal at later times is caused mainly by neutrals is supported by this order of magnitude calculation. The fact that also no discrete lines are present after 80 microseconds leads to the conclusion that the plasma is in a burn-out state.

REFERENCES

1. M. A. Babikin, P. P. Gavrin, E. K. Zavoiskii, L. I. Rudakov, and V. A. Skoryupin, Zh. Eksperim. i Teor. Fiz. 41, 1597 (1964). (Engl. Transl.: Soviet Phys. JETP 20, 1073 (1965)).

2. E. C. Field and B. D. Fried, Phys. Fluids 7, 1937 (1964).

3. R. Betchov, Phys. Fluids Suppl., 1967, S 17.

4. O. Buneman, Phys. Rev., 115, 503 (1959).

5. L. J. Demeter, ERL University of California, Berkeley, Technical Report AFAL-TR-65-119 (June, 1965).

6. L. Heroux and H. E. Hinteregger, The Rev. of Scient. Instr. 31, March 1960.

7. C. N. Burrous, A. J. Lieber and V. T. Zaviantseff, The Rev. of Scient. Instr. 38, 1477, (1967).

8. V. T. Zaviantseff, ERL Report No. 66-12, Univ. of Calif., Berkeley, California (June 11, 1966).

9. H. K. Forsen, ERL Report No. 65-16, Univ. of Calif., Berkeley, California (June 7, 1965).

10. A. J. Lichtenberg, S. Sesnic, and A. W. Trivelpiece, Phys. Rev. Letters 13, 387 (1964).

11. A. J. Lichtenberg, S. Sesnic, and A. W. Trivelpiece, Univ. of Calif., Berkeley, ERL Report No. 64-28 (August 17, 1964).

12. Plasma Diagnostic Techniques, Edited by Richard H. Huddlestone and Stanley L. Leonard, Academic Press New York, London, page 388 (1965).

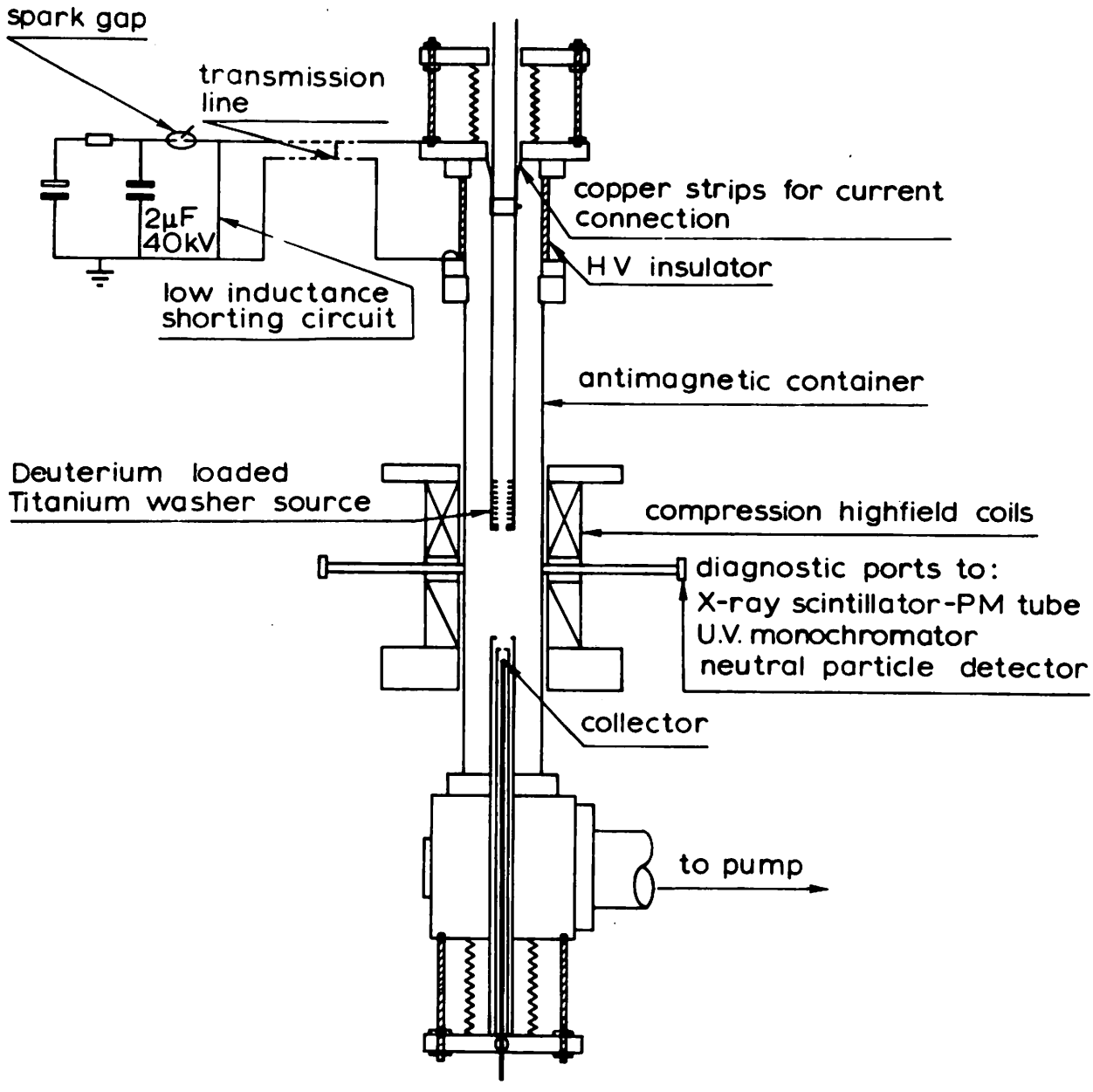

Fig. 1. Schematic picture of the experiment.

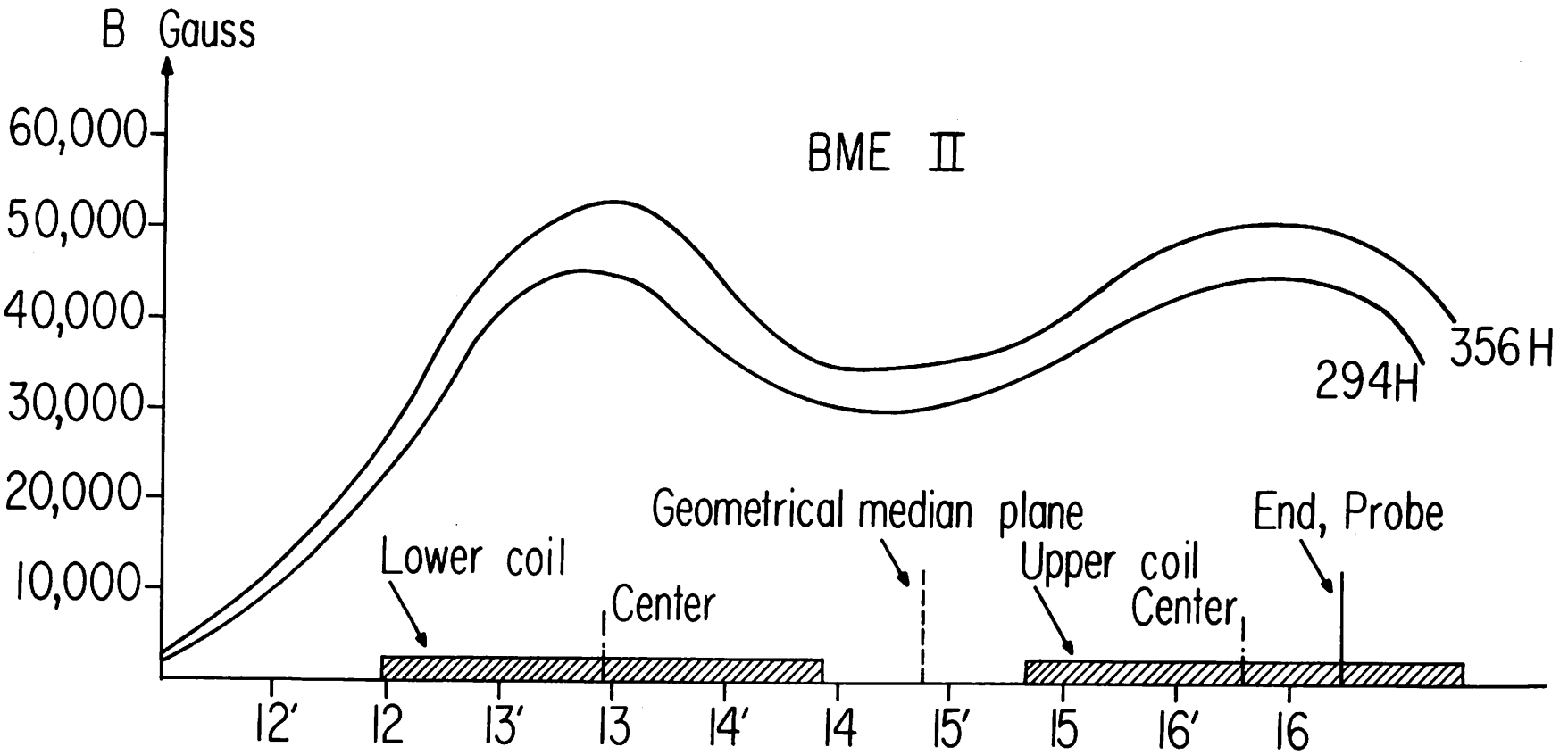

Fig. 2. BME II magnetic field shape.

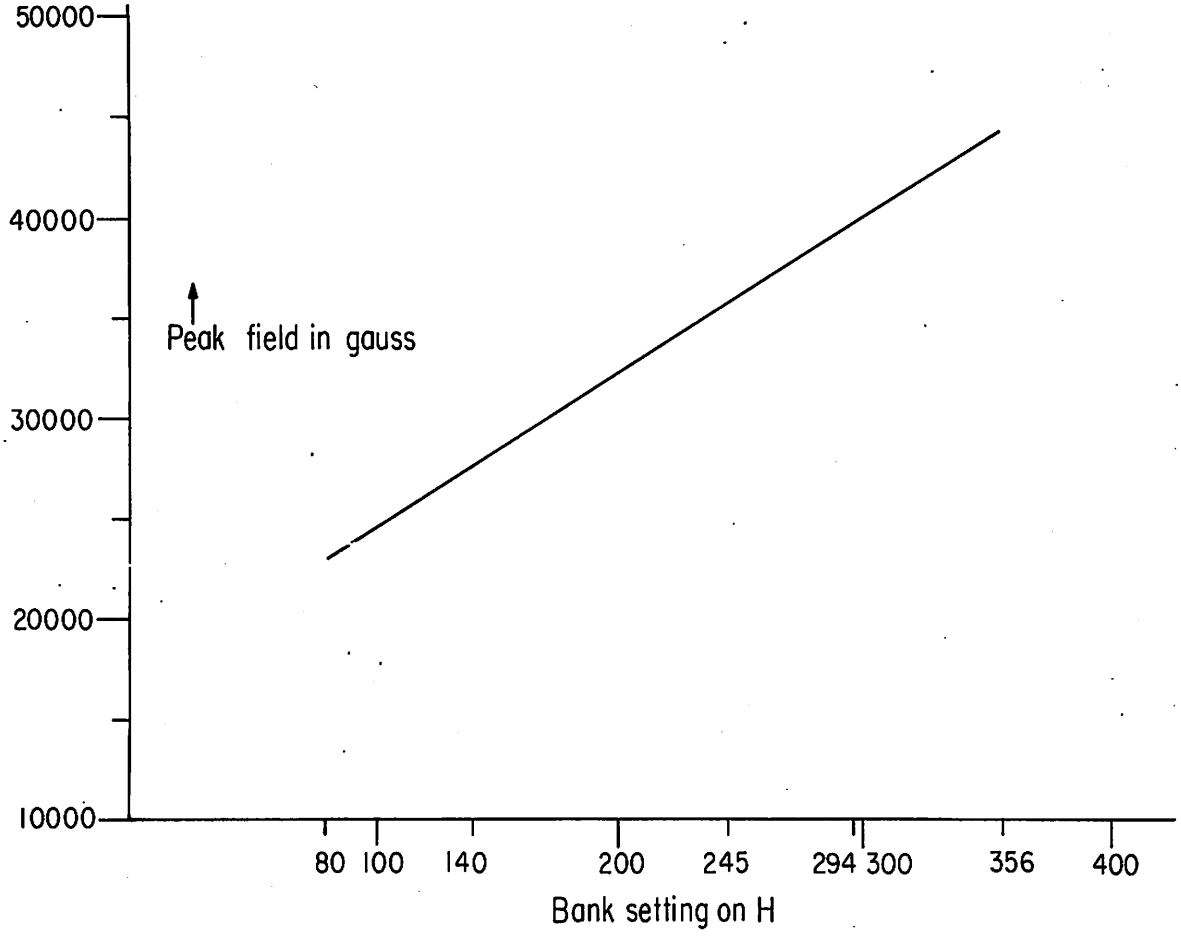

Fig. 3. BME II maximum field in Gauss vs bank setting.

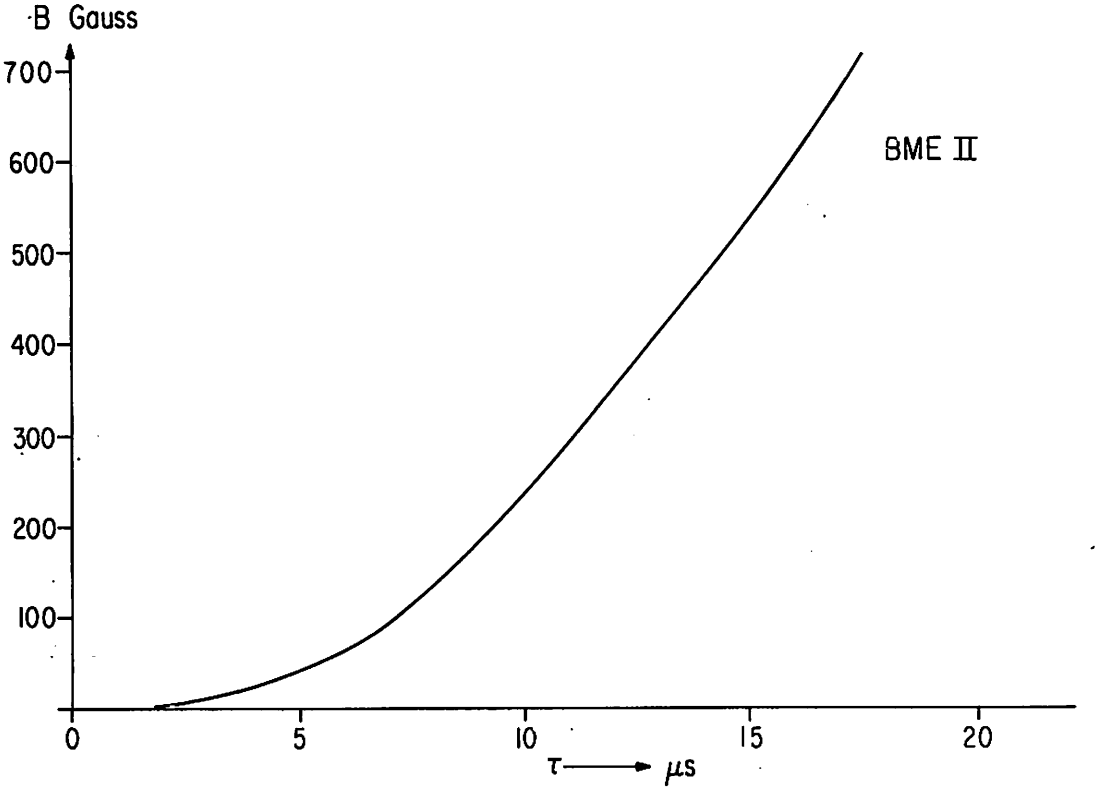

Fig. 4a) BME II field in Gauss from 0 - 17 μs.

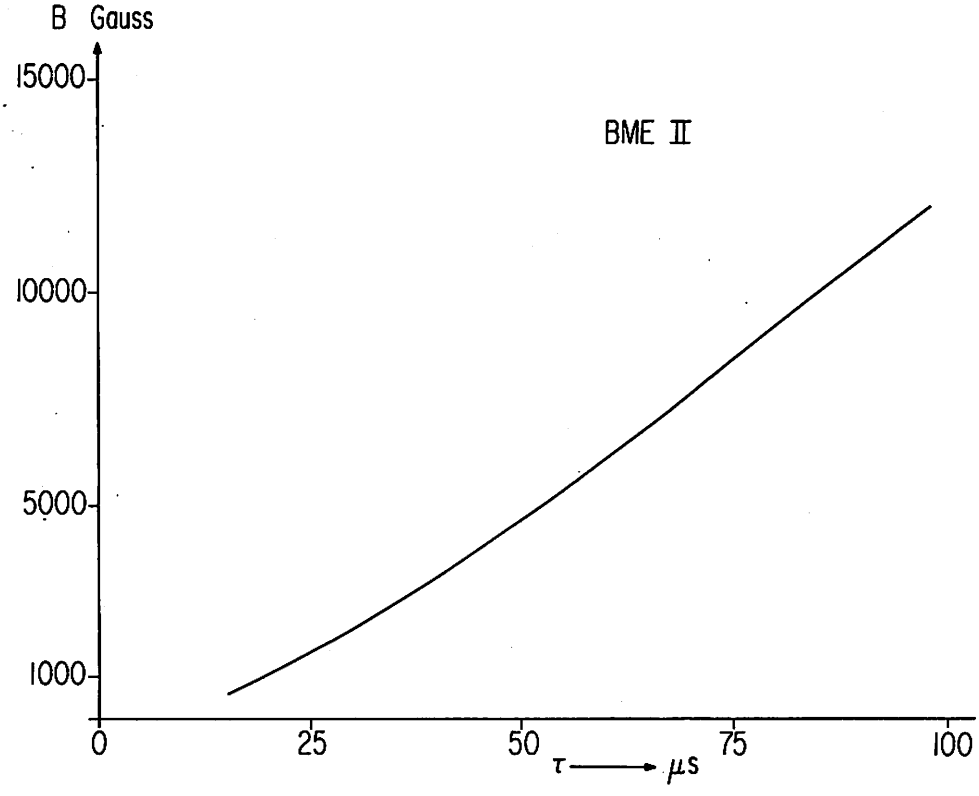

Fig. 4b) BME II field in Gauss from 15 - 100 μs.

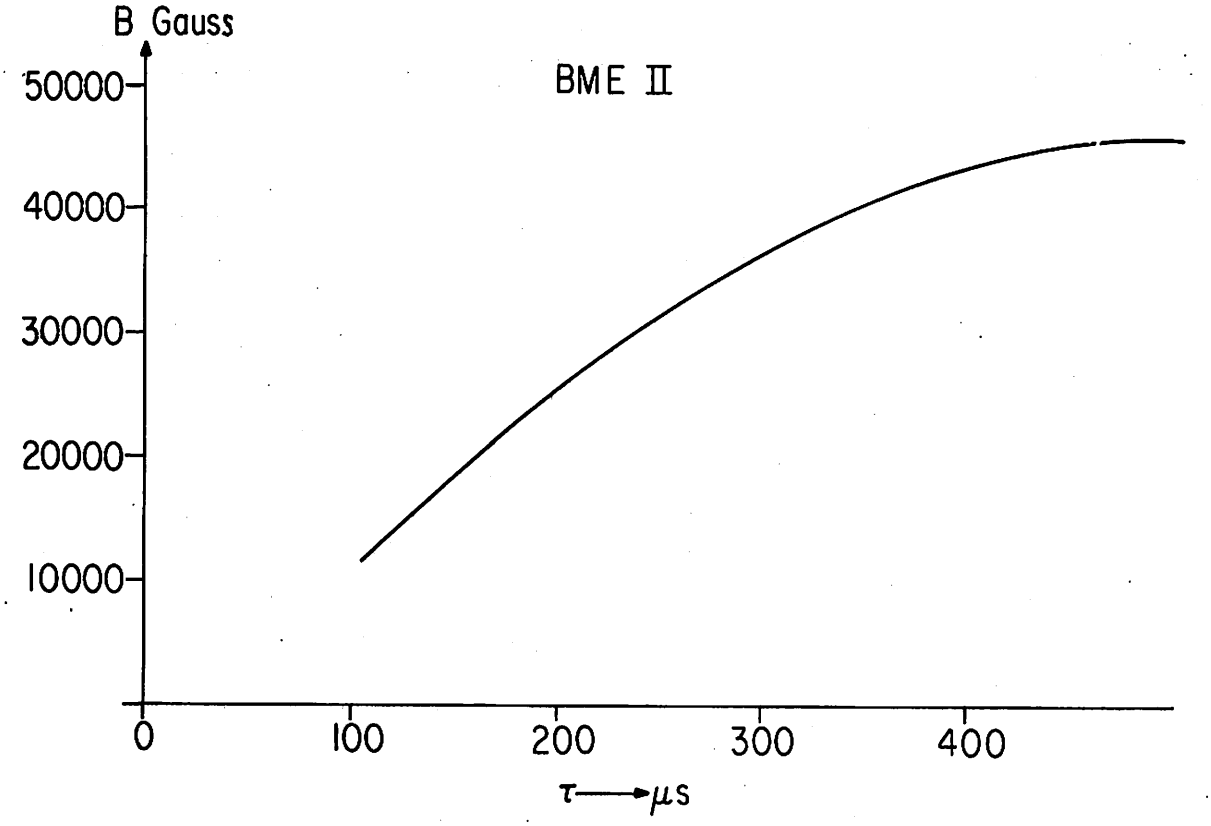

Fig. 4c) BME II field in Gauss from 100 - 500 μs.

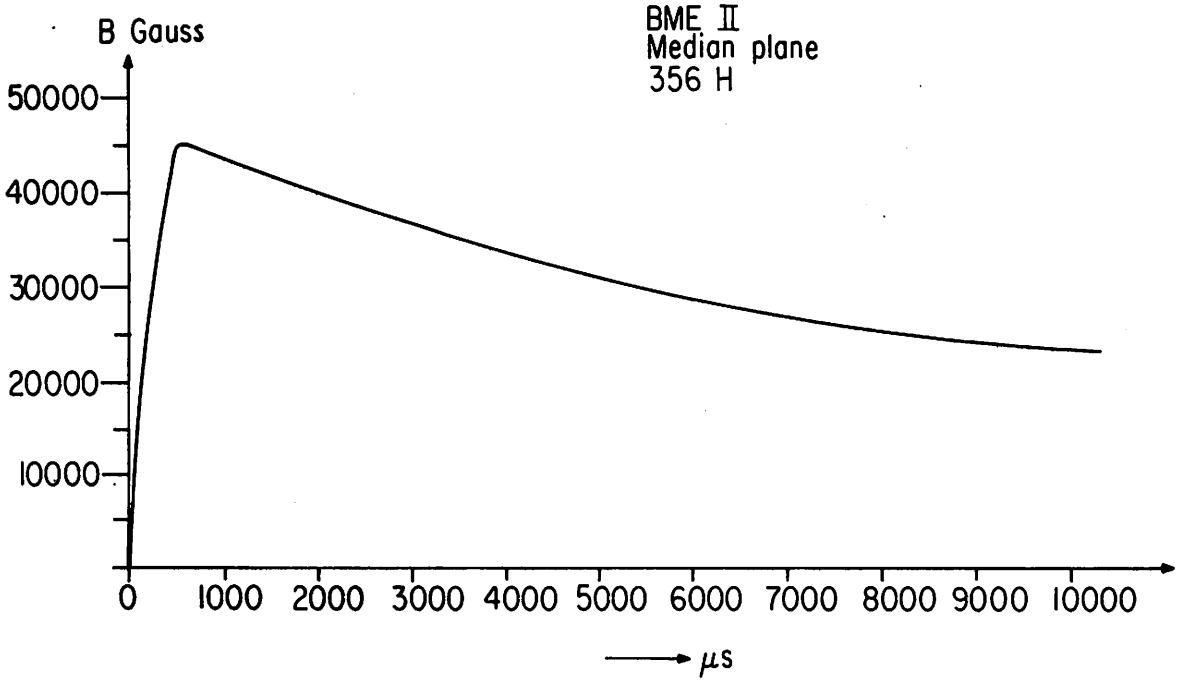

Fig. 4d) BME II field in Gauss from 0 - 10 ms.

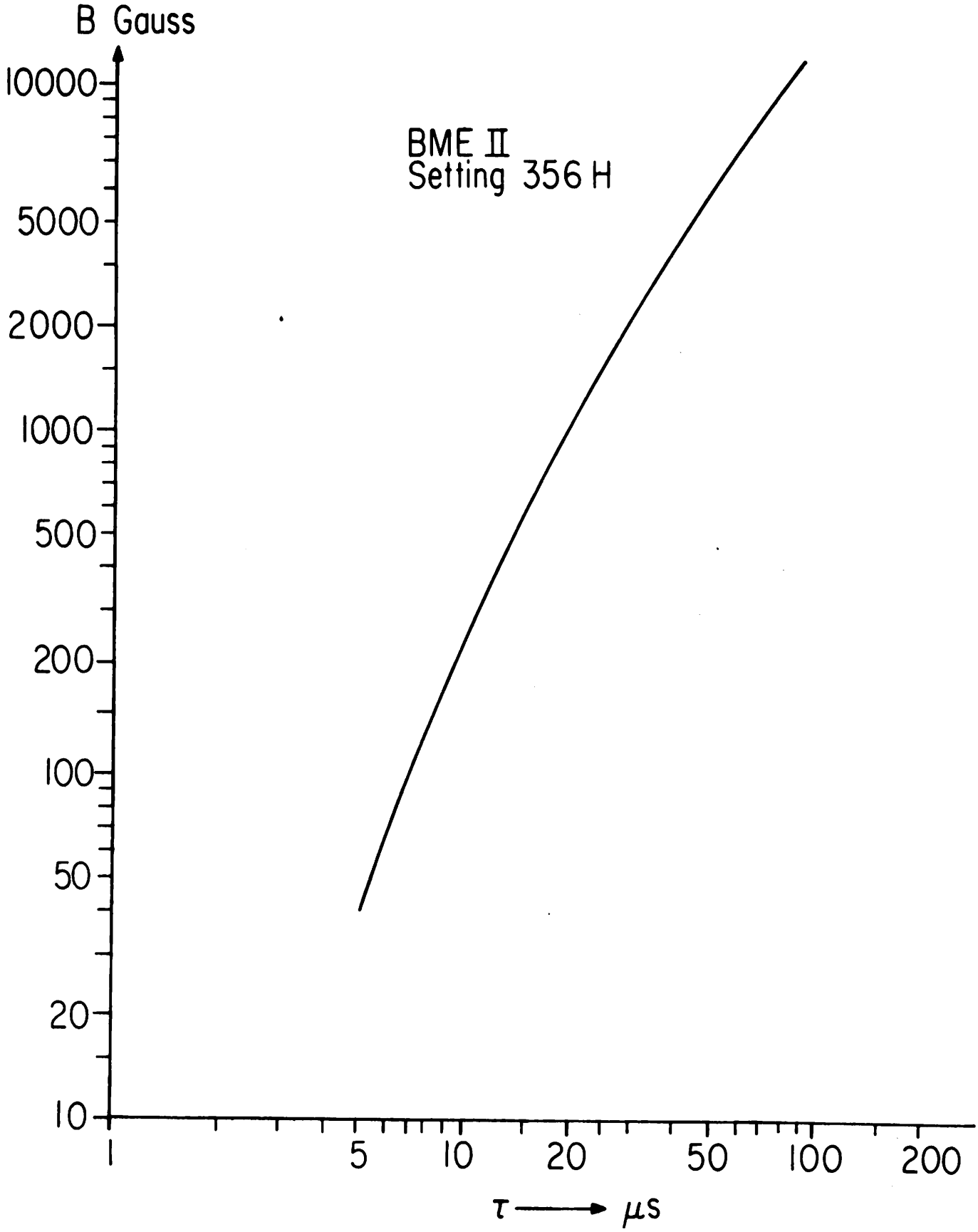

Fig. 4e) logarithmic plot of BME II field in Gauss from 5 - 100 μs.

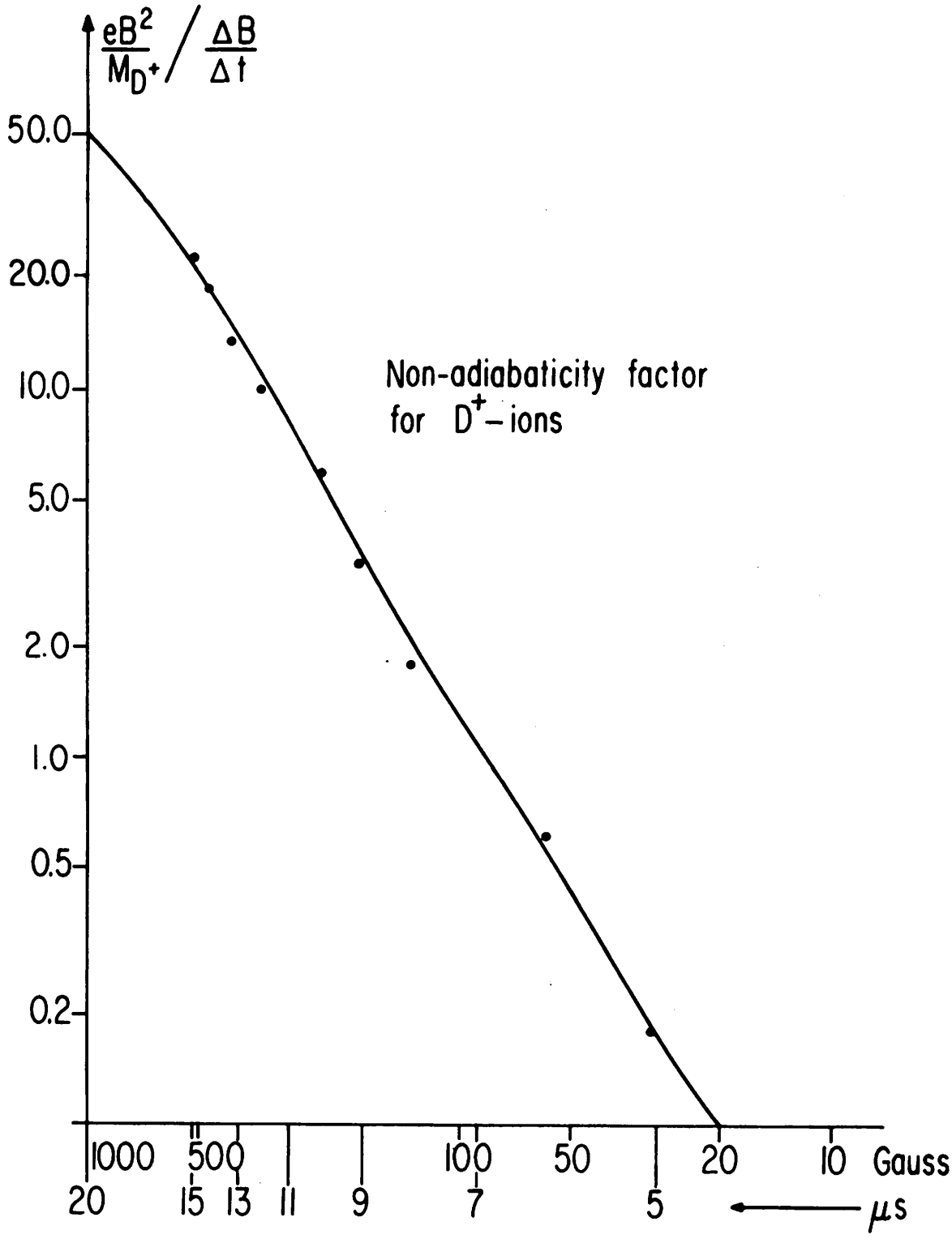

Fig. 5. Non-adiabaticity parameter for D^+-ions vs B and t.

parameter: $\frac{e^2B}{m} \frac{\Delta B}{\Delta t}$.

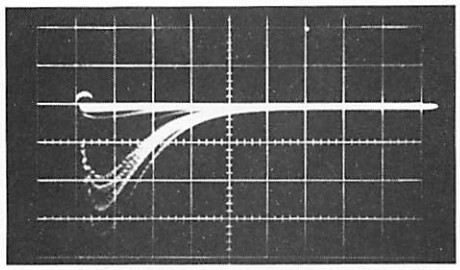

Fig. 6. Li iodine scintillations single pulses from a plutonium 238, beryllium stable isotope. Neutrons between 3 and 5 MeV. Stilbeen thermalizer. PM tube 2100 Volts over 1000 Ω.

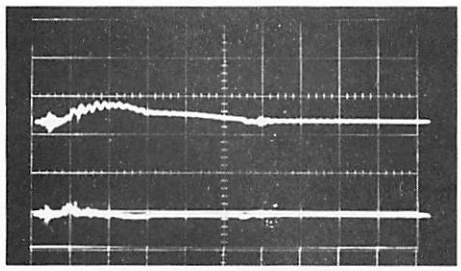

Fig. 7. Duration of plasma current in the presence of a rising B-field, measured by a Rogowsky coil. Sweep speed 5 μsec/div.

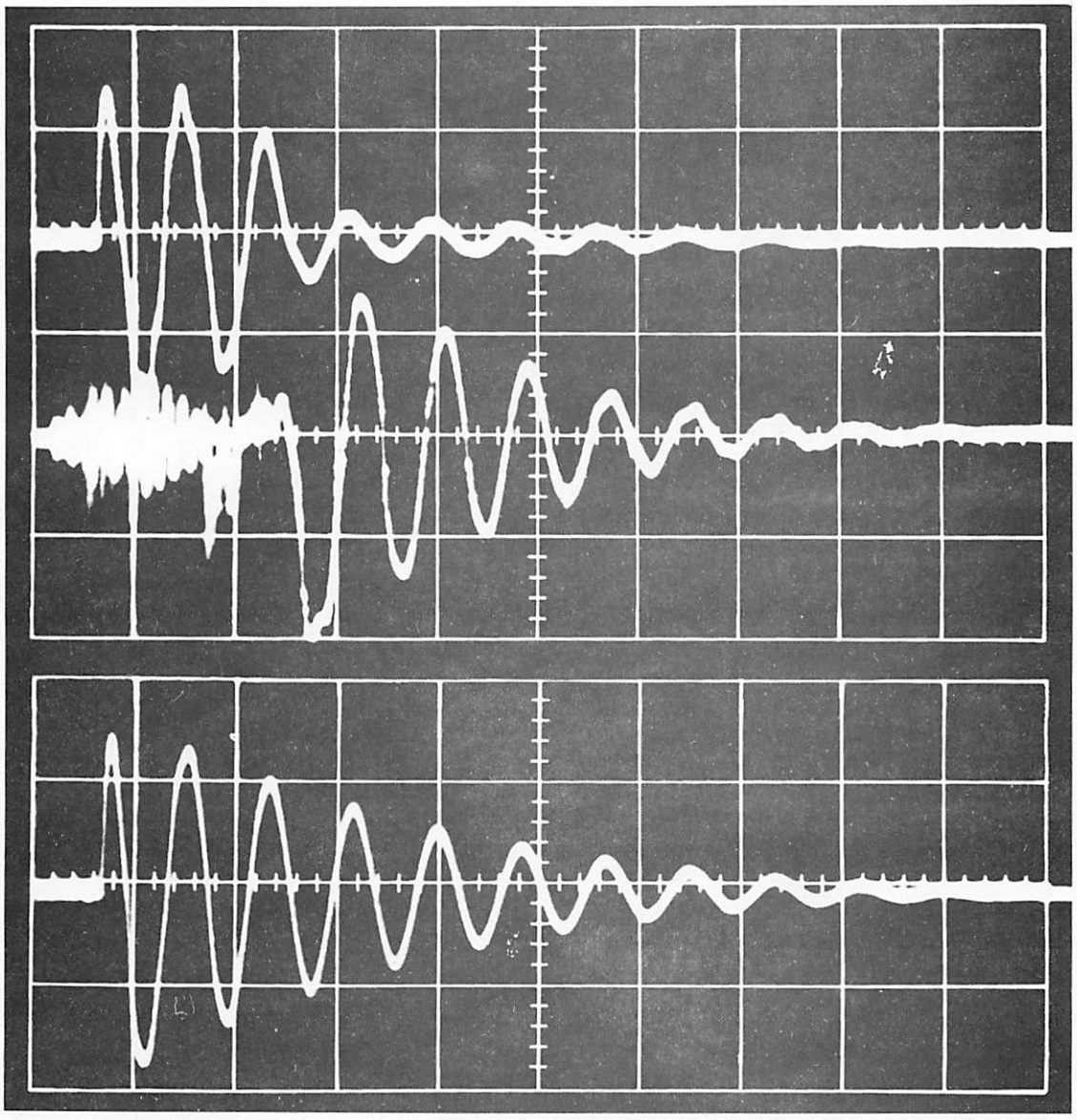

Fig. 8. Oscillating voltages and current through the plasma. Sweep speed: 5 μsec/div. Lower trace: voltage damping out without plasma; gain 2 kV/div. Upper and middle traces, respectively, voltage and current in the presence of plasma. Current 0.5 kA/div.

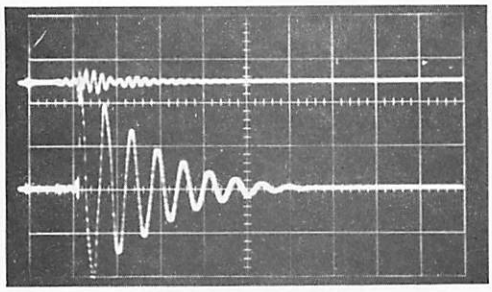

a) Capacitor discharging through short without plasma injection. Lower trace: unperturbed damped, voltage oscillation; sweep speed: 5 microseconds per div; gain 1 kV per div. Upper trace: Rogowsky coil signal with no current, some pickup. Capacitor voltage: 20 kV; frequency 335 kCs.

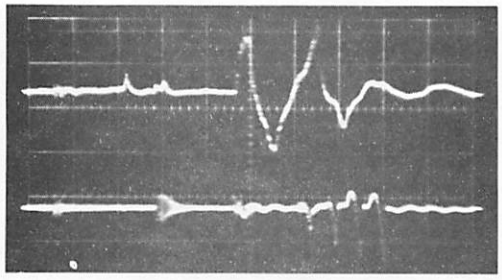

b) Capacitor discharging in the presence of plasma. Upper trace: voltage; sweep speed 2 microseconds per div. Gain 2 kV per div. Lower trace: current 25 kA per div. Notice asymmetry in the current. Negative peaks correspond with electrons hitting the capacitor electrode. Capacitor at 22.5 kV.

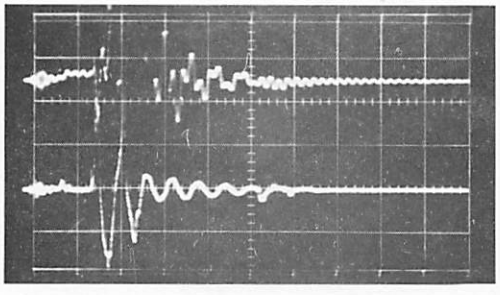

c) Upper trace: current with larger gain, 600 Amp per div; sweep speed 5 microseconds per div. Lower trace: voltage 1 kV per div. It can be seen that, apart from some high frequency pickup, the current and voltage have almost an Ohmic relation during the first oscillations, with resistance of the order of 1 Ohm.

Fig. 9.

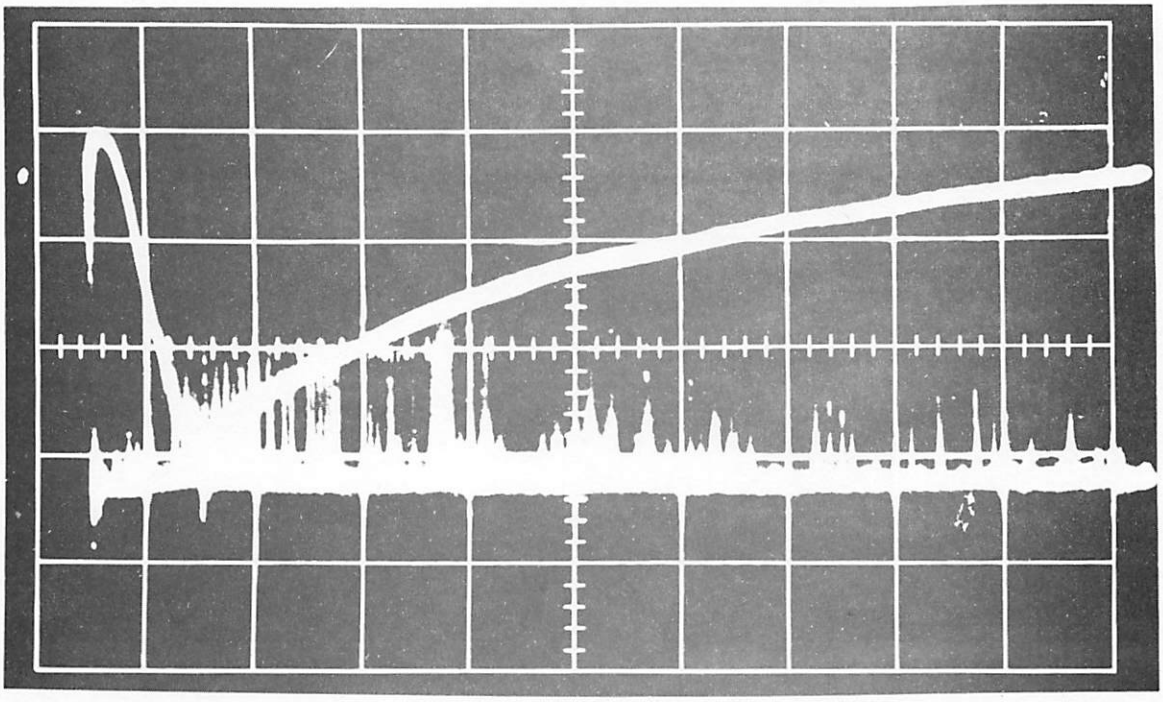

a) Electron cyclotron radiation and X-rays without excitation. Upper trace cyclotron radiation: 2 mV/div. Lower trace X-rays: 20 mV/div. Sweep speed: 500 μsec/div.

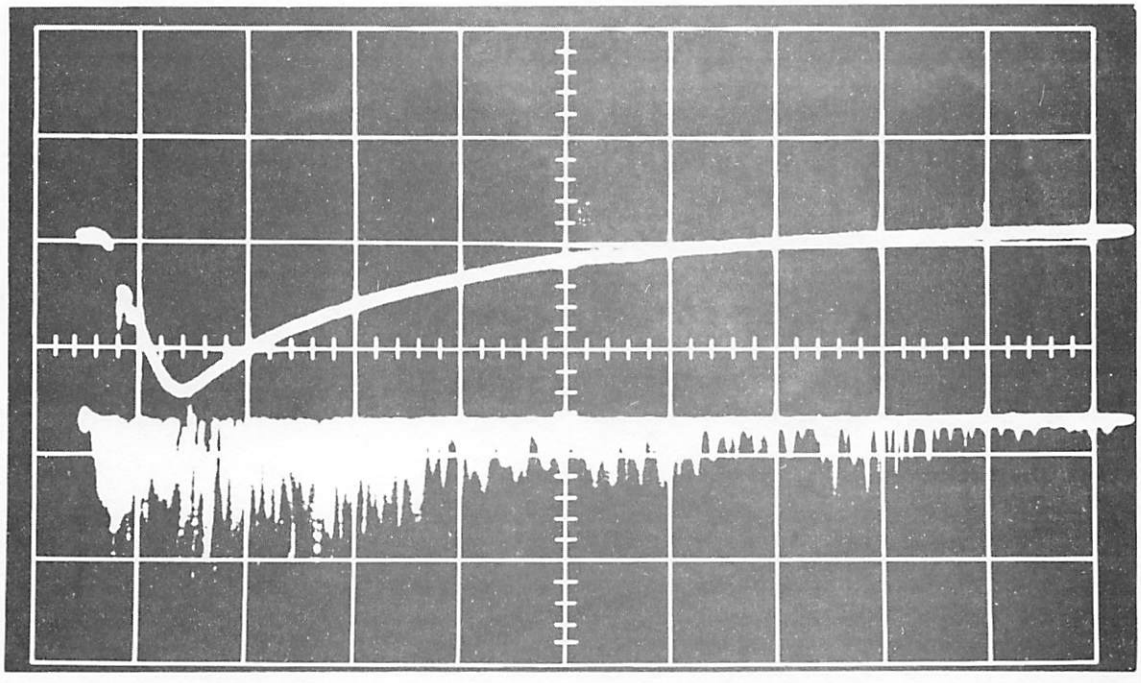

b) Electron cyclotron radiation and X-rays with 240 kc/s oscillations. Upper trace: 20 mV/div. Lower trace: 0.2 V/div. Sweep speed: 500 μsec/div. Notice the increase in both signals by the capacitor discharge.

Fig. 10.

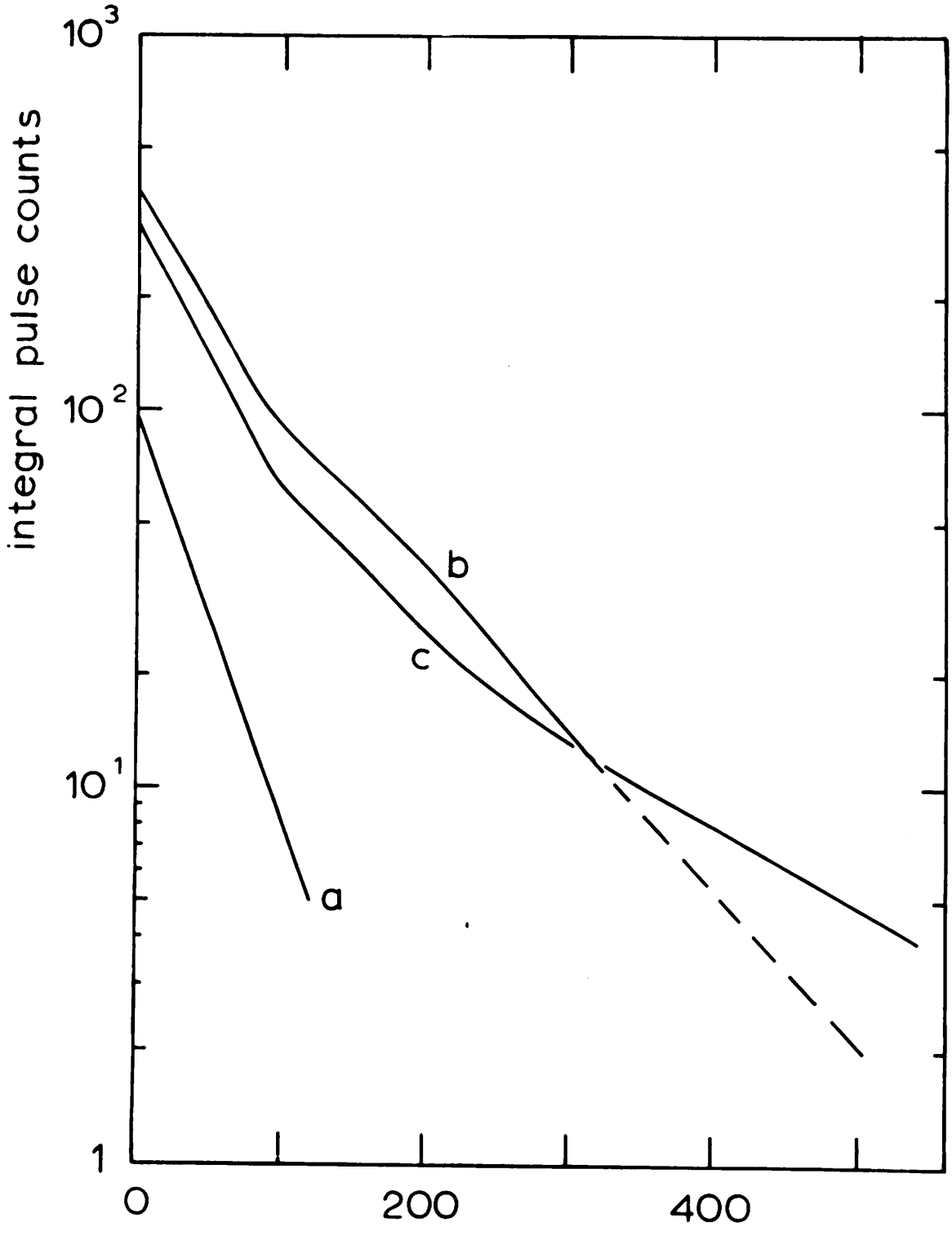

Fig. 11. Integral pulse counts of X-rays. a: without additional heating, temperature 50 keV; b: with 240 kc/s oscillations, temperatures of two Maxwellians 140 and 60 keV; c: with 340 kc/s oscillations, temperatures of 240 and 60 keV.

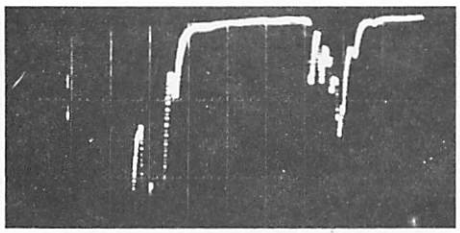

Fig. 12. 127° ion-analyzer signal showing small burst of ions lost through lower mirror at 140 μsec. The energies of the escaping ions should correspond with 1000 eV. The largest part of the escaping particles is lost between 0 and 60 μsec. This part is off screen in this photo. Time scale 20 μsec/div. Vertical axis 0.1 V/div. Single ion signals approximately 0.05 V.

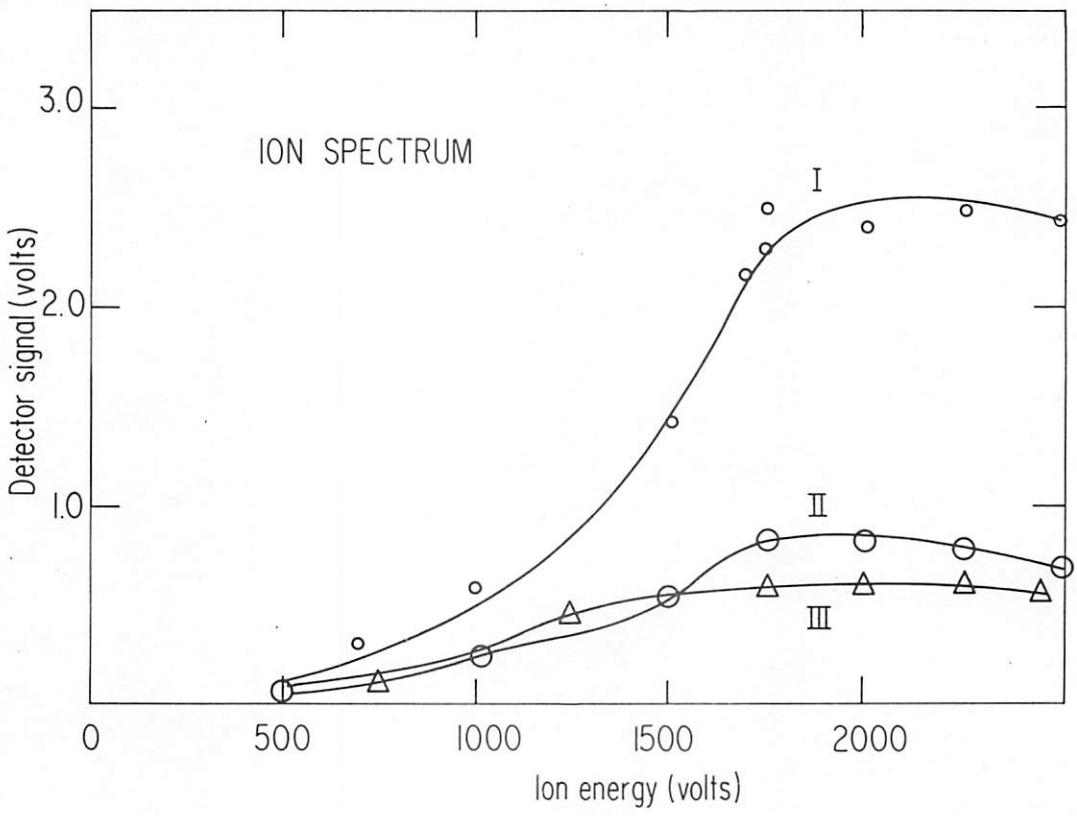

Fig. 13. Ion energy measurements end-on under various conditions with 127° ion-analyzer. Time of measurement 10-15 μsec after source start.
Curve I: with capacitor 240 kc/s and compression field.
Curve II: without capacitor and with magnetic compression field.
Curve III: without capacitor; no magnetic field.
Notice: a) the absence of signals below 500 eV.
b) the capacitor discharge increases the ion flux lost by a factor of 2 to 3. The shape, however, is essentially unaltered.

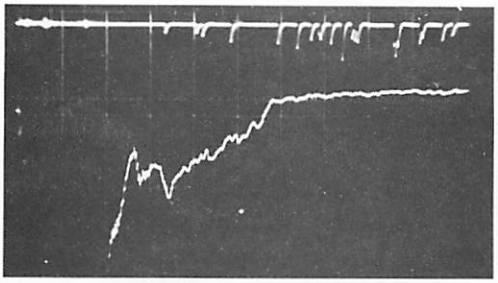

Fig. 14. Lower trace: Lyman alpha line at high gain; sweep speed 20 microseconds per div. Notice the second maximum near 60 microseconds. Intensity ratio of first to second maximum is approximately 10 to 1. Upper trace: X-rays. Signals are recorded with capacitor discharge. Notice the early X-ray emission.

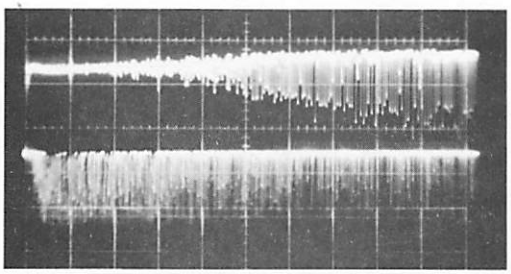

Fig. 15. Upper trace: Bendix signal through a small pinhole; sweep speed 500 microseconds per div. The signal is saturated up to 3 milliseconds, degrading into single spikes later. Lower trace: X-ray emission. Peak magnetic field is 45 kG.

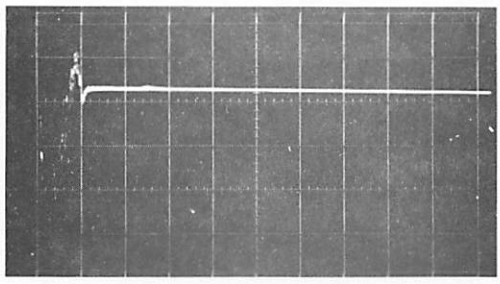

a) Electron and ion collector current due to plasma gun. Collector biased at - 45 V. Sweep speed: 20 microseconds per div. Notice electrons dominating at first; later ion current dominates. There is no magnetic field.

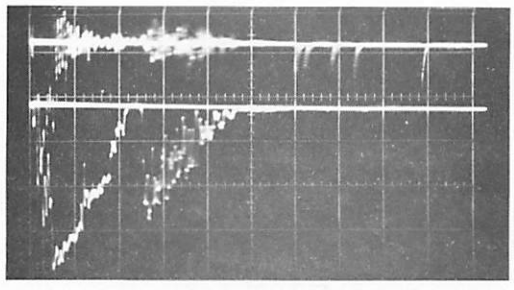

b) First and second maximum in electron current. Collector is biased at + 160 V; sweep speed: 20 microseconds per div.

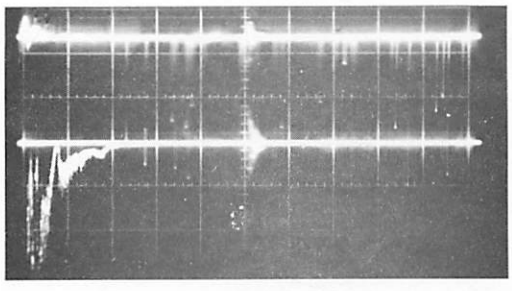

c) Collector current showing several ionization maxima. Sweep speed is 100 microseconds per div; collector biased at 160 V to suppress ions. Traces b) and c) are taken together.

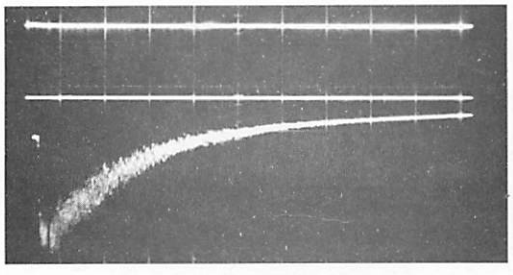

d) The actual loss current of the trapped and compressed plasma. Collector biased at 160 V to suppress ions. Sweep speed: 1000 microseconds per div. Peak magnetic field for Fig. 4d was 45 kG.

Fig. 16.

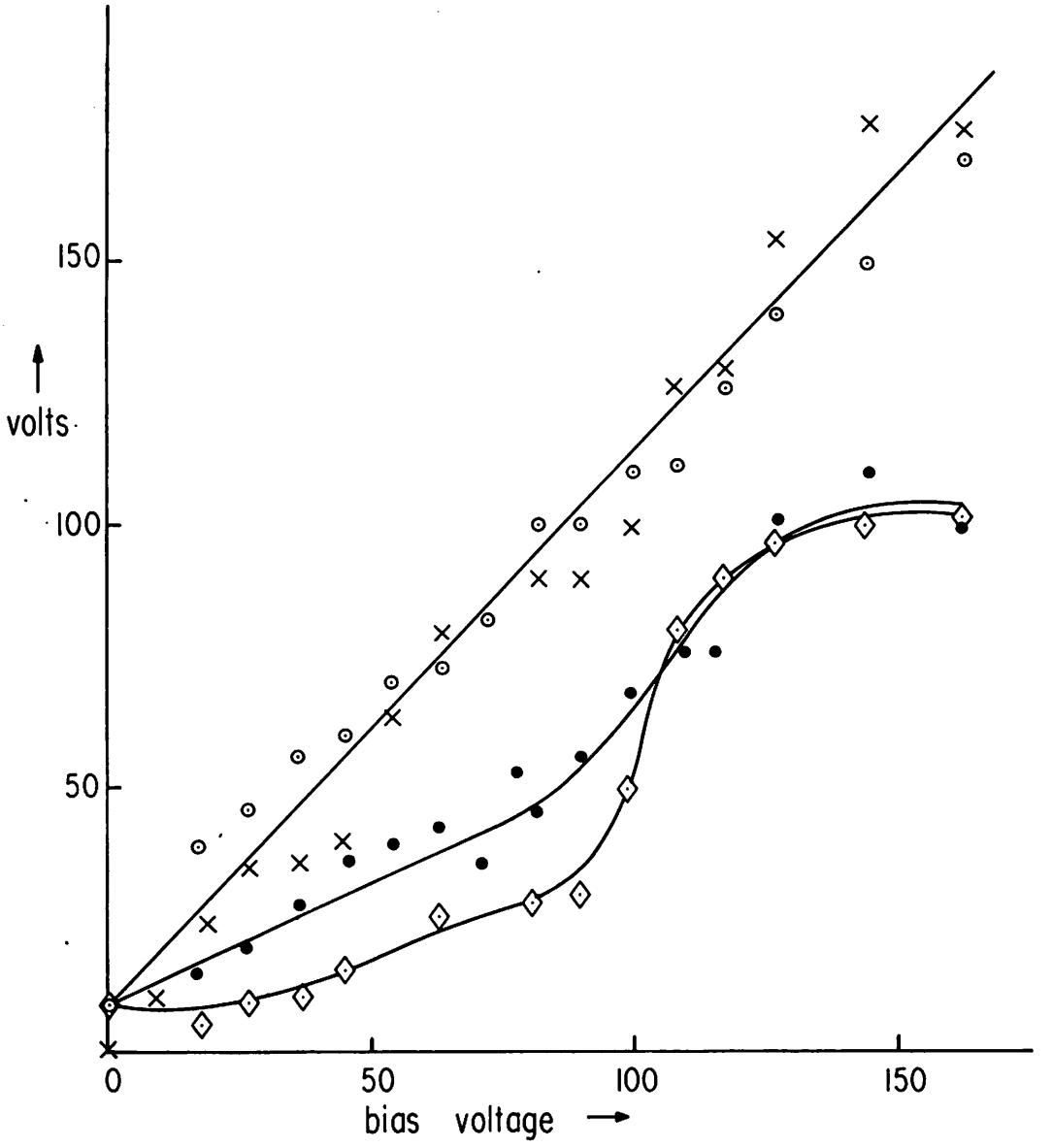

Fig. 17. Electron loss currents at biased collector below lower mirror. Measurements are taken across 200 Ohm.
0 : peak at 20 microseconds without capacitor) no difference
x : peak at 20 microseconds with capacitor)
. : peak at 60 microseconds without capacitor
⊡: peak at 60 microseconds with capacitor
Notice: energies are more peaked near 100 eV with capacitor. The data have been obtained with 340 kc/s and capacitor charged up to 23 kV.

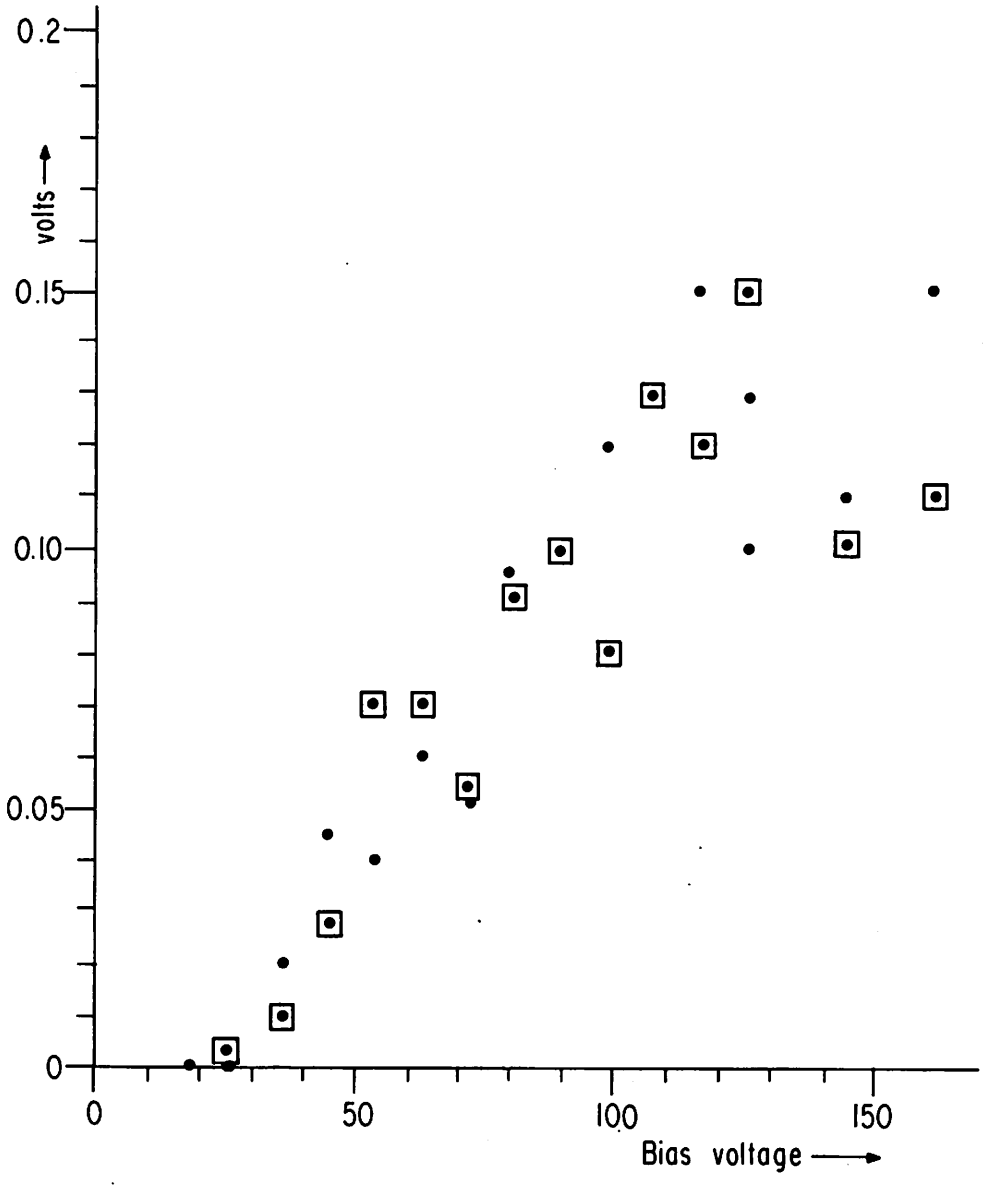

Fig. 18. The loss currents near maximal compression time (450 microseconds) plotted versus positive bias voltage of the same collector as for Fig. 17. Data have been taken across 200 Ohm.
. : with capacitor discharge
⊡: without capacitor discharge